Physics Letters B 683 (2010) 134–139

Contents lists available at ScienceDirect

Physics Letters B

www.elsevier.com/locate/physletb

# Relativistic description of BCS–BEC crossover in nuclear matter

Bao Yuan Sun [a,b], Hiroshi Toki [b,a], Jie Meng [c,a,d,e,f,*]

[a] School of Physics and State Key Laboratory of Nuclear Physics and Technology, Peking University, 100871 Beijing, China
[b] Research Center for Nuclear Physics (RCNP), Osaka University, Ibaraki, Osaka 567-0047, Japan
[c] School of Physics and Nuclear Energy Engineering, Beihang University, 100191 Beijing, China
[d] Department of Physics, University of Stellenbosch, Stellenbosch, South Africa
[e] Institute of Theoretical Physics, Chinese Academy of Sciences, 100080 Beijing, China
[f] Center of Theoretical Nuclear Physics, National Laboratory of Heavy Ion Accelerator, 730000 Lanzhou, China

ARTICLE INFO

*Article history:*
Received 15 April 2009
Received in revised form 30 September 2009
Accepted 11 November 2009
Available online 11 December 2009
Editor: J.-P. Blaizot

*Keywords:*
Pairing correlation
Nuclear matter
Relativistic pairing theory
Bare nucleon–nucleon interaction
Di-neutron spatial correlation
BCS–BEC crossover

ABSTRACT

We study theoretically the di-neutron spatial correlations and the crossover from superfluidity of neutron Cooper pairs in the $^1S_0$ pairing channel to Bose–Einstein condensation (BEC) of di-neutron pairs for both symmetric and neutron matter in the microscopic relativistic pairing theory. We take the bare nucleon–nucleon interaction Bonn-B in the particle–particle channel and the effective interaction PK1 of the relativistic mean-field approach in the particle–hole channel. It is found that the spatial structure of neutron Cooper pair wave function evolves continuously from BCS-type to BEC-type as density decreases. We see a strong concentration of the probability density revealed for the neutron pairs in the fairly small relative distance around 1.5 fm and the neutron Fermi momentum $k_{Fn} \in [0.6, 1.0]$ fm$^{-1}$. However, from the effective chemical potential and the quasiparticle excitation spectrum, there is no evidence for the appearance of a true BEC state of neutron pairs at any density. The most BEC-like state may appear at $k_{Fn} \sim 0.2$ fm$^{-1}$ by examining the density correlation function. From the coherence length and the probability distribution of neutron Cooper pairs as well as the ratio between the neutron pairing gap and the kinetic energy at the Fermi surface, some features of the BCS–BEC crossover are seen in the density regions, 0.05 fm$^{-1}$ $< k_{Fn} <$ 0.7 (0.75) fm$^{-1}$, for the symmetric nuclear (pure neutron) matter.



Pairing correlations, as collective phenomena found in various systems as liquid $^3$He, superconductors, atomic nuclei, and ultracold atomic gases, play a crucial role in the fermion systems. When an attractive interaction between two fermions is weak, i.e., the pairing gap is much smaller than the Fermi energy, partner fermions can be treated as a delocalized Cooper pair with large overlap as described in the Bardeen–Cooper–Schrieffer (BCS) theory [1], displaying a strong correlation in the momentum space. If an interaction is sufficiently strong, fermion pairs become a spatially compact bosonic bound state and undergo Bose–Einstein condensation (BEC), showing a strong correlation in the coordinate space. As the strength of attractive interaction between two fermions increases, the pairing phenomenon evolves from BCS to BEC state. The transition between them, often referred as BCS–BEC crossover, brings a new insight into the pairing phenomenon. Although the BCS and BEC limits are physically quite different, the evolution between them was found to be smooth and continuous [2–4].

In nuclear physics, neutron pairs are expected to be strongly correlated at some density. There are rather general reasons to expect that di-neutron correlations in low-density nuclear matter should be significant. It is well known that the bare nucleon–nucleon interaction in the $^1S_0$ channel leads to a virtual state around zero energy characterized by the large negative scattering length $a \approx -18.5 \pm 0.4$ fm [5]. This implies a very strong attraction between two neutrons in the spin singlet state, although the neutron–neutron interaction is not strong enough to form a two-body bound state in free space. Furthermore, theoretical predictions suggest that at around 1/10 of the nuclear saturation density $\rho_0$, the $^1S_0$ pairing gap may take a considerably larger value than that around $\rho_0$ [6,7].

Weakly bound neutron-rich nuclei provide optimum circumstance to study di-neutron correlations in the low-density region, where the density around surface is unsaturated and the couplings to the continuum spectra play an essential role [8–12]. Originally, the possible existence of a di-neutron near the surface of nuclei was predicted by Migdal in 1972 [13]. In his work, it was shown that although di-neutron is unbound in vacuum, it may form a bound state in a potential well if there is a single-particle level with energy close to zero. Subsequently, plenty of theoretical investigation based on either schematic or microscopic models

* Corresponding author at: School of Physics and Nuclear Energy Engineering, Beihang University, 100191 Beijing, China.
*E-mail addresses:* toki@rcnp.osaka-u.ac.jp (H. Toki), mengj@pku.edu.cn (J. Meng).

0370-2693/$ – see front matter 
doi:10.1016/j.physletb.2009.11.065

displayed a clear signature of the strong di-neutron correlation in the ground state, not only in light closed-shell core plus $2n$ or $4n$ nuclei [14,8,15–17,12,18,19], but also in medium or heavy neutron-rich nuclei [20–23], as well as in infinite nuclear matter [24,25]. It has been revealed that the concentration of small sized Cooper pairs in the surface of superfluid nuclei is a quite generic feature [23]. In fact, such a di-neutron correlation is in connection with the BEC-like behavior in infinite nuclear matter at low densities. Recently, a strong low-lying dipole strength distribution of the two-neutron halo nucleus $^{11}$Li has been observed experimentally [26]. The spectrum was reproduced well by a three-body model with a strong di-neutron correlation [27,28].

Theoretical and experimental progress on di-neutron correlations in weakly bound nuclei has stimulated lots of renewed interests in possible BCS–BEC crossover of di-neutron pairs. The systematical analysis was performed in nuclear matter by using the bare force given by a superposition of three Gaussian functions, the finite-range Gogny interaction, and the zero-range contact interaction without or with medium polarization effects [29–31]. It was shown that the correlations between two neutrons get large as density decreases, and the spatial structure of neutron Cooper pairs changes. As a result, the BCS–BEC crossover occurs in the uniform matter at low densities. In particular, for the screened pairing interaction, a di-neutron BEC state is formed in symmetric matter at around $0.001\rho_0$. The above results have been confirmed by a further study, where the change of sign of the density correlation function at low momentum transfer is taken as a criterion of the BCS–BEC crossover [32]. In addition, the coexistence of BCS- and BEC-like spatial structures of neutron pairs was studied in the halo nucleus $^{11}$Li as well [33]. It has been shown that as the distance between the center of mass of the two neutrons and the core increases, the two-particle wave function changes from the weak coupling BCS regime to the strongly correlated BEC regime. This result clearly confirms that a strong di-neutron correlation between the valence neutrons is present on the surface of the nucleus.

Details of the effective nucleon–nucleon force in nuclei are as yet not completely clarified since most of the experimental data in nuclear spectroscopy are not very sensitive to the details of the nucleon–nucleon force. Hence, in most of investigations on nuclear pairing correlations, for convenience, the effective nuclear forces such as zero-range contact forces or finite-range Gogny force, are used in the particle–particle ($pp$) channel. The effective interactions in relativistic mean-field (RMF) theory are also used in the $pp$ channel [34,35]. In order to obtain reasonable values for the gap parameter, one has to introduce an effective factor [35]. Hence, the properties of Cooper pairs and BCS–BEC crossover from these existing phenomenological calculations need further check. Furthermore, in the low-density limit, the interaction in the $pp$ channel approaches the bare nucleon–nucleon interaction. Therefore, it is interesting to use the realistic bare nucleon–nucleon interaction in the $pp$ channel and explore the BCS–BEC crossover at low densities.

In this Letter, the di-neutron spatial correlations in the $^1S_0$ channel will be studied in a relativistic pairing theory, i.e., relativistic Hartree–Fock–Bogoliubov (RHFB) theory [34], with the realistic bare nucleon–nucleon interaction, i.e., the relativistic Bonn potential [36], in the $pp$ channel. Then the BCS–BEC crossover phenomenon and the possibility of di-neutron BEC states at low densities will be discussed.

The RMF theory [37] has attracted lots of attentions during the last decades due to its great success in describing both nuclear matter and finite nuclei near or far from the stability line [38,39]. In the RHFB theory, meson fields are treated dynamically beyond the mean-field theory to provide the pairing field via the anomalous Green's functions [34]. In the case of infinite nuclear matter, the Dirac–Hartree–Fock–Bogoliubov equation reduces to the usual BCS equation. For the $^1S_0$ channel, the pairing gap function $\Delta(p)$ is

$$\Delta(p) = -\frac{1}{4\pi^2}\int_0^\infty v_{pp}(k,p)\frac{\Delta(k)}{2E_k}k^2\,dk, \tag{1}$$

where $v_{pp}(k,p)$ is the matrix elements of nucleon–nucleon interaction in the momentum space for the $^1S_0$ pairing channel, and $E_k$ is the quasiparticle energy,

$$E_k = \sqrt{(\varepsilon_k-\mu)^2+\Delta(k)^2}, \tag{2}$$

with the single-particle energy $\varepsilon_k$, and the chemical potential $\mu$. The corresponding normal and anomalous density distribution function have the form,

$$\rho_k = \frac{1}{2}\left[1-\frac{\varepsilon_k-\mu}{E_k}\right], \qquad \kappa_k = \frac{\Delta(k)}{2E_k}. \tag{3}$$

The single-particle energy $\varepsilon_k$ follows from the standard RMF approach [37],

$$\varepsilon_k = \Sigma_0 + \sqrt{k^2+M^{*2}}, \tag{4}$$

where the scalar mass $M^* = M+\Sigma_S$, $\Sigma_0$ the vector potential and $\Sigma_S$ the scalar potential. For nuclear matter with given baryonic density $\rho_b$ and isospin asymmetry $\zeta = (\rho_n-\rho_p)/\rho_b$, the above equations can be solved by a self-consistent iteration method with no-sea approximation.

The relativistic Bonn potential is used in the $pp$ channel, which has a proper momentum behavior determined by the scattering data up to high energies [36]. It is defined as the sum of one-boson-exchange (OBE) of the several mesons $\phi = \sigma,\omega,\pi,\rho,\eta,\delta$. The matrix elements $v_{pp}(\boldsymbol{k},\boldsymbol{p})$ is

$$v_{pp}(\boldsymbol{k},\boldsymbol{p}) = \sum_\phi \frac{\eta_\phi}{2\varepsilon_k^*\varepsilon_p^*}A_\phi(\boldsymbol{k},\boldsymbol{p})D_\phi(\boldsymbol{q}^2)F_\phi^2(\boldsymbol{q}^2), \tag{5}$$

where $\varepsilon_k^*$ is the effective single-particle energy

$$\varepsilon_k^* = \sqrt{k^2+M^{*2}}. \tag{6}$$

$D_\phi(\boldsymbol{q}^2)$ is a meson propagator with momentum transfer $\boldsymbol{q}=\boldsymbol{k}-\boldsymbol{p}$, and $F_\phi(\boldsymbol{q}^2)$ is a form factor of monopole type,

$$D_\phi(\boldsymbol{q}^2) = \frac{1}{\boldsymbol{q}^2+m_\phi^2}, \qquad F_\phi(\boldsymbol{q}^2) = \frac{\Lambda_\phi^2-m_\phi^2}{\boldsymbol{q}^2+\Lambda_\phi^2}, \tag{7}$$

with $m_\phi$ the mass of meson, and $\Lambda_\phi$ the cutoff parameter. $\eta_\phi$ and $A_\phi(\boldsymbol{k},\boldsymbol{p})$ are the vertex functions of the relativistic Bonn potential. For the $^1S_0$ pairing channel, the matrix element $v_{pp}(k,p)$ is just the average of $v_{pp}(\boldsymbol{k},\boldsymbol{p})$ over the angle $\theta$ between the vectors $\boldsymbol{k}$ and $\boldsymbol{p}$,

$$v_{pp}(k,p) = \int_0^\pi v_{pp}(\boldsymbol{k},\boldsymbol{p})\sin\theta\,d\theta. \tag{8}$$

Bonn-B potential [36] is adopted for $v_{pp}(k,p)$. For the mean-field calculation in the particle–hole ($ph$) channel, the effective interaction PK1 [40] is used, since the results do not depend sensitively on various other parameter sets [41].

To investigate the spatial structure of neutron Cooper pairs, it is useful to look into its wave function represented as a function of the relative distance $r = |\boldsymbol{r}_1-\boldsymbol{r}_2|$ between the pair partners. The Cooper pair wave function in momentum space $\Psi_{\rm pair}(k)$ is just the

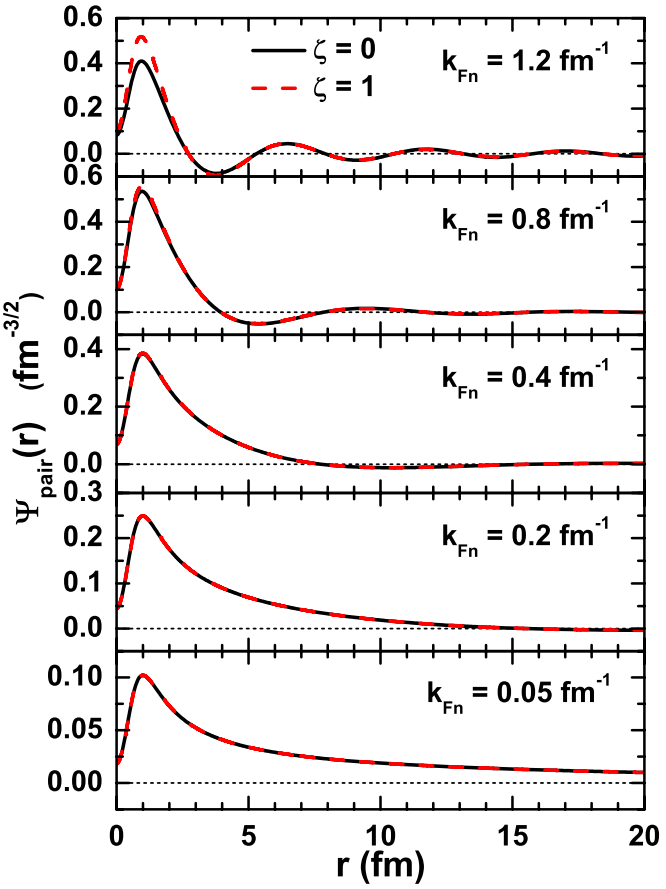


**Fig. 1.** Neutron Cooper pair wave function in coordinate space $\Psi_{\rm pair}(r)$ as a function of the relative distance $r$ between the pair partners at several neutron Fermi momenta $k_{Fn}$ in symmetric nuclear matter ($\zeta = 0$, black solid lines) and pure neutron matter ($\zeta = 1$, red dashed lines). Notice the different scales on the ordinate in the various panels. (For interpretation of the references to color in this figure legend, the reader is referred to the web version of this Letter.)

anomalous density $\kappa_k$, and its coordinate representation is deduced from the Fourier transform,

$$\Psi_{\rm pair}(r) = \frac{C}{(2\pi)^3}\int \kappa_k e^{i\boldsymbol{k}\cdot\boldsymbol{r}}\, d\boldsymbol{k}, \tag{9}$$

where $C$ is the constant determined from the normalization condition

$$\int \left|\Psi_{\rm pair}(r)\right|^2 r^2\, dr = 1. \tag{10}$$

In Fig. 1, the wave function of the neutron Cooper pairs $\Psi_{\rm pair}(r)$ is shown as a function of the relative distance $r$ between the pair partners at different neutron Fermi momenta $k_{Fn}$. Nearly identical results are given for the symmetric nuclear matter ($\zeta = 0$) and pure neutron matter ($\zeta = 1$), except for $k_{Fn} = 1.2$ fm$^{-1}$, where a larger amplitude of the first peak is obtained in pure neutron matter.

The radial shape of $\Psi_{\rm pair}(r)$ changes as density decreases. When $k_{Fn} = 1.2$ fm$^{-1}$ and 0.8 fm$^{-1}$, the profile of the wave function $\Psi_{\rm pair}(r)$ shows an oscillatory behavior convoluted by a decreasing exponent, which is a typical behavior of BCS state. A significant amplitude outside the first node is observed. As density goes down to $k_{Fn} = 0.4$ fm$^{-1}$ and 0.2 fm$^{-1}$, the wave function becomes compact in shape and the oscillation disappears, resembling the strong coupling BEC-like bound state. This indicates that a possible BCS–BEC crossover may occur in uniform matter at such low densities. At very dilute density of $k_{Fn} = 0.05$ fm$^{-1}$, the wave function becomes more extended again and approaches to zero slowly.

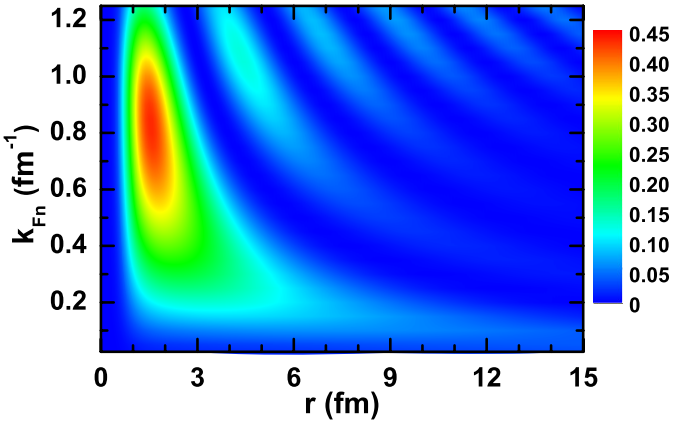


**Fig. 2.** A two-dimensional plot for the probability density $r^2|\Psi_{\rm pair}(r)|^2$ of the neutron Cooper pairs as a function of the neutron Fermi momentum $k_{Fn}$ and the relative distance $r$ between the pair partners in symmetric nuclear matter.

Turning ones attention to short distance $r$, a suppressed amplitude around $r = 0$ fm is displayed at all densities, that is attributed to the strong repulsive contribution of $v_{pp}(k, p)$ at high momentum. In addition, for all the densities a peak appears around $r = 1.0$ fm, around which it has been confirmed that the pairing potential in the coordinate space $v_{pp}(r)$ reaches the strongest attraction [25].

Furthermore, it is noteworthy that the evolution of the wave function with the density in Fig. 1 is similar to those for the proton–neutron pairing in Ref. [42] in which a true bound state of deuterons is predicted in the low-density limit. Thus, one needs to explore whether a true di-neutron BEC bound state appears in nuclear matter as well.

To illustrate a clear picture of di-neutron correlations, a two-dimensional plot for the probability density $r^2|\Psi_{\rm pair}(r)|^2$ of the neutron Cooper pairs for symmetric nuclear matter is shown in Fig. 2, as a function of the neutron Fermi momentum $k_{Fn}$ and the relative distance $r$ between the pair partners. A strong concentration of the probability density is revealed for the pair partners in a surprisingly small relative distance of $r \sim 1.5$ fm in the density region about 0.6 fm$^{-1} < k_{Fn} < 1.0$ fm$^{-1}$. This behavior has the same physical essence as the di-neutron configuration in the surface of superfluid nuclei as discussed in Refs. [22,23,33]. As a matter of fact, the pairing gap at the Fermi surface $\Delta_{Fn} \equiv \Delta(k_{Fn})$ also depends strongly on $k_{Fn}$, and achieves a large value together with probability density in such a density region.

When the Fermi momentum is close to the saturation density, the probability density $r^2|\Psi_{\rm pair}(r)|^2$ indicates a considerable distribution outside the first peak and extends to a large distance $r$. This phenomenon is well understood by the orthogonalization of the wave function for the paired particles with the remaining particles due to the Pauli principle, which expels the Cooper pair wave function outside. As density decreases, these amplitudes die out gradually and a compact structure appears at about 0.2 fm$^{-1} < k_{Fn} < 0.5$ fm$^{-1}$. While going to lower densities of $k_{Fn} < 0.2$ fm$^{-1}$, the probability density has a very small value and exhibits a long tail at large relative distance $r$. This behavior may be responsible for the appearance of halo structure in several neutron-rich nuclei at far distance away from the center [9,10,28].

Since a strong di-neutron correlation is revealed at low densities from the Cooper pair wave function and the corresponding probability density, it is deserved to study the possibility of Bose–

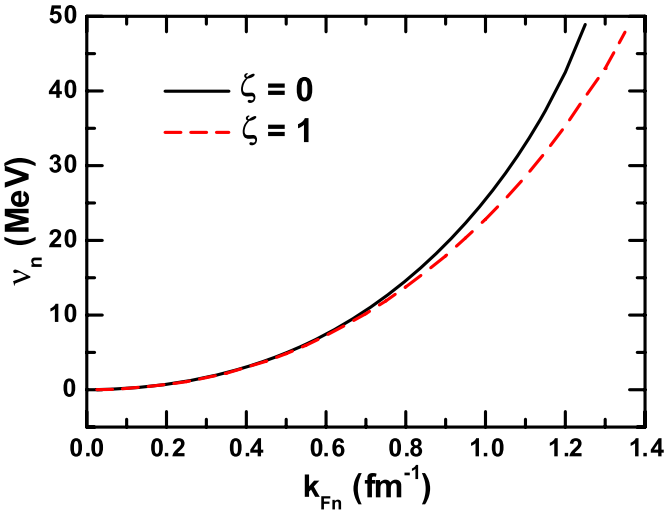


**Fig. 3.** Effective neutron chemical potential $\nu_n$ as a function of the neutron Fermi momentum $k_{Fn}$ in symmetric nuclear matter (black solid line) and pure neutron matter (red dashed line). (For interpretation of the references to color in this figure legend, the reader is referred to the web version of this Letter.)

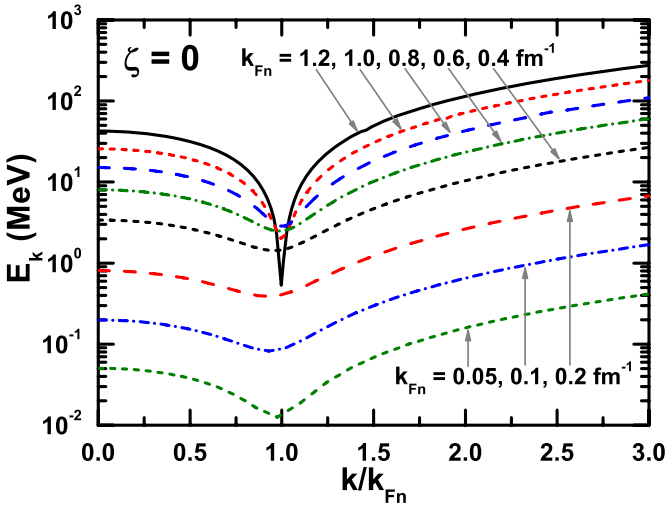


**Fig. 4.** Neutron quasiparticle excitation energy $E_k$ as a function of the ratio of the neutron momentum to the Fermi momentum $k/k_{Fn}$ at different neutron Fermi momenta $k_{Fn}$ in symmetric nuclear matter.

Einstein condensation and the BCS–BEC crossover phenomenon of di-neutrons as density decreases.

In the whole debate around BCS–BEC transition the chemical potential $\mu$ plays a central role. It has been proved in an easy way that the gap in Eq. (1) together with the normal and anomalous density distribution function in Eq. (3) goes over into the Schrödinger-like equation for the neutron pair wave function $\Psi_{\text{pair}}(k)$, and the corresponding energy eigenvalue is related to the chemical potential [3]. In the case of the RMF approach, it is expressed as

$$2e(k)\Psi_{\text{pair}}(k) + \frac{(1-2\rho_k)}{4\pi^2}\int_0^\infty v_{pp}(k,p)p^2\,dp\,\Psi_{\text{pair}}(p) = 2\nu_n\Psi_{\text{pair}}(k), \tag{11}$$

where $e(k)$ is the neutron kinetic energy,

$$e(k) = \sqrt{k^2 + M^{*2}} - M^*. \tag{12}$$

$\nu_n$ is the effective neutron chemical potential obtained by deducting momentum independent part from the chemical potential $\mu_n$,

$$\nu_n = \mu_n - \Sigma_0 - M^*, \tag{13}$$

which could be regarded as half of the "binding energy" of a Cooper pair. At transition from the BCS regime of large overlapping neutron Cooper pairs to the BEC regime with true di-neutron bound states, $\nu_n$ is supposed to turn from positive to negative values.

In Fig. 3, the effective neutron chemical potential $\nu_n$ as a function of the Fermi momentum $k_{Fn}$ in nuclear matter is given. The values of $\nu_n$ decrease monotonically in both symmetric nuclear matter and pure neutron matter as density goes down, and come very close to zero at dilute area but never turn negative. It is then expected in this case that a true di-neutron bound state does not occur in nuclear matter, but the transition to BEC is very close in the low-density limit.

The qualitative changes in the quasiparticle excitation spectrum have been suggested as another clear distinction between the BCS and BEC limits [43], i.e., the momentum corresponding to the minimum in the excitation spectrum will shift from finite momentum in the BCS limit to zero momentum in the BEC limit, and the value of the pairing gap also changes from $\Delta$ in the BCS limit to $\sqrt{\mu^2+\Delta^2}$ in the BEC limit.

In Fig. 4, the quasiparticle excitation spectra $E_k$ is shown as functions of $k/k_{Fn}$ at several neutron Fermi momenta in symmetric nuclear matter. The minimum of $E_k$ always appears around the Fermi momentum $k_{Fn}$ for all the densities, i.e., the minimum of $E_k$ approaches to zero momentum with the corresponding Fermi momentum but become zero only when $k_{Fn}=0$. Similar results are obtained for the pure neutron matter as well. Therefore, from the quasiparticle excitation spectrum, there is no evidence for the appearance of a true BEC bound state of neutron pairing with the realistic bare nucleon–nucleon interaction Bonn-B at any density, in agreement with that from the effective chemical potential $\nu_n$.

The analogies with other low-density Fermi systems, such as ultracold atomic gases, could be used to study the BCS–BEC crossover in nuclear matter as well. The neutron density correlation function is such a quantity that gives prominence to the relative strength between the mean field and the pairing field, which is defined as [44,32]

$$D(q) = I_\kappa(q) - I_\rho(q). \tag{14}$$

At zero momentum transfer, the normal and anomalous density contributions $I_\rho$ and $I_\kappa$ respectively read

$$I_\rho(0) = \frac{1}{\pi^2\rho_n}\int_0^\infty \rho_k^2 k^2\,dk, \tag{15}$$

$$I_\kappa(0) = \frac{1}{\pi^2\rho_n}\int_0^\infty \kappa_k^2 k^2\,dk, \tag{16}$$

and they satisfy the sum rule

$$I_\rho(0) + I_\kappa(0) = 1. \tag{17}$$

The change of sign of the density correlation function at low momentum transfer is taken as a criterion of the BCS–BEC crossover [44], although further study argued that this criterion can be trusted only at small isospin asymmetry [32].

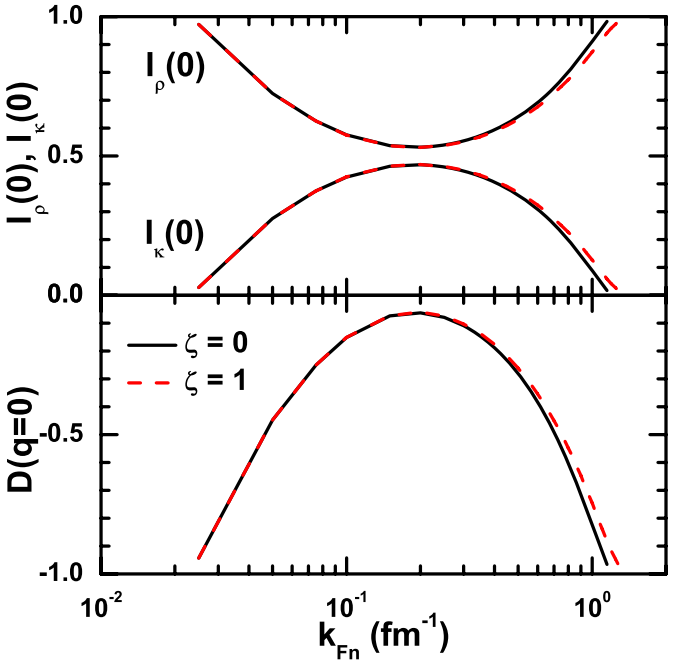


**Fig. 5.** Zero-momentum transfer density correlation function $D(q=0)$ and its normal and anomalous density contributions, $I_\rho(0)$ and $I_\kappa(0)$, as a function of the neutron Fermi momentum $k_{Fn}$ in symmetric nuclear matter (black solid lines) and pure neutron matter (red dashed lines). (For interpretation of the references to color in this figure legend, the reader is referred to the web version of this Letter.)

In Fig. 5, the density correlation functions at zero-momentum transfer $D(0)$ and its normal and anomalous density contributions, $I_\rho(0)$ and $I_\kappa(0)$, are shown as functions of $k_{Fn}$ in nuclear matter. With decreasing density, $I_\rho(0)$ first drops down from 1.0, reaches a minimum at $k_{Fn} \sim 0.2$ fm$^{-1}$ ($\rho_n/\rho_0 \sim 10^{-3}$), and then increases to 1.0 again. While $I_\kappa(0)$ gives an opposite trend and has no contribution when approaching to either the saturation density or the dilute density. This leads to a peak for the density correlation function $D(0)$ around $k_{Fn} = 0.2$ fm$^{-1}$, where the most BEC-like state may appear. It is consistent with the result of $\Psi_{\rm pair}(r)$ shown in Fig. 1, where the wave function behaves like a spatially compact bound state at $k_{Fn} = 0.2$ fm$^{-1}$. Because the anomalous density contribution $I_\kappa(0)$ is always smaller than the normal one $I_\rho(0)$, the density correlation function never changes sign at all. According to the criterion mentioned above, di-neutrons are not in BEC state but just in the transition region between BCS and BEC regimes, that verifies the conclusion from the effective chemical potential and the quasiparticle excitation spectrum.

To describe the BCS–BEC crossover quantitatively, lots of characteristic quantities have been introduced [29,30]. The rms radius of the neutron Cooper pair $\xi_{\rm rms}$, i.e., coherence length, is a straightforward measure to evaluate the pairing size,

$$\xi_{\rm rms}^2 = \langle r^2 \rangle = \frac{\int |\Psi_{\rm pair}(r)|^2 r^4\, dr}{\int |\Psi_{\rm pair}(r)|^2 r^2\, dr} = \frac{\int_0^\infty (\frac{\partial}{\partial k}\kappa_k)^2 k^2\, dk}{\int_0^\infty \kappa_k^2 k^2\, dk}, \tag{18}$$

which can be calculated either from the Cooper pair wave function $\Psi_{\rm pair}(r)$ or from $\kappa_k$ in the momentum space. The latter one is more suitable since the gap equation is solved in momentum space. The coherence length $\xi_{\rm rms}$ has a solid meaning even in the strong coupling BEC case or the crossover region between BCS and BEC. For comparison, the average inter-neutron distance $d_n \equiv \rho_n^{-1/3}$ is taken into account. If $\xi_{\rm rms} > d_n$, the neutron Cooper pair is interpreted as an extended BCS-like pair, otherwise it will be considered as a compact BEC-like pair.

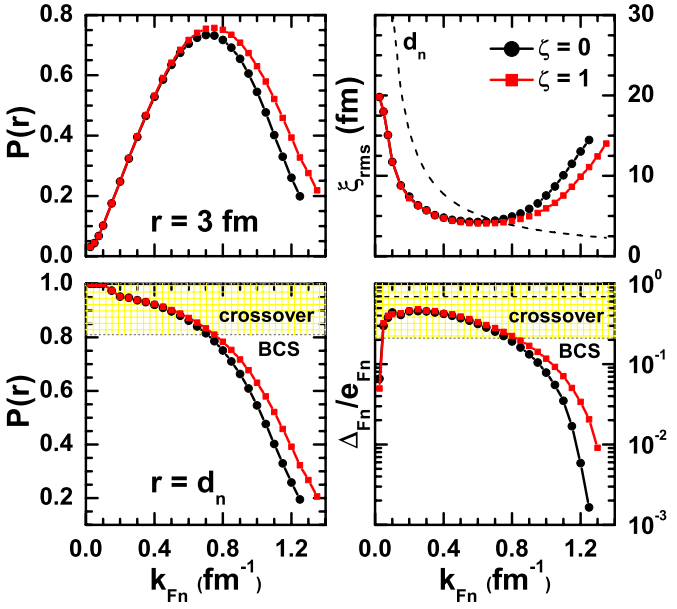


**Fig. 6.** Probability $P(r)$ for the partner neutrons correlated within $r = 3$ fm (upper-left panel) and the average inter-neutron distance $r = d_n$ (lower-left panel) as a function of the neutron Fermi momentum $k_{Fn}$. The black line with filled circle is for the symmetric nuclear matter and the red line with filled square is for the pure neutron matter. The corresponding rms radius $\xi_{\rm rms}$ of the neutron Cooper pair is plotted in upper-right panel in comparison with the average inter-neutron distance $d_n$ (the dashed curve). The ratio $\Delta_{Fn}/e_{Fn}$ between the neutron pairing gap at the Fermi surface $\Delta_{Fn}$ and the neutron Fermi kinetic energy $e_{Fn}$ as a function of $k_{Fn}$ is plotted in lower-right panel. The referred BCS–BEC crossover regions (yellow grid) and the unitary limit (dashed line) from the regularized pairing model [29,30] for $P(d_n)$ and $\Delta_{Fn}/e_{Fn}$ are given respectively. (For interpretation of the references to color in this figure legend, the reader is referred to the web version of this Letter.)

The coherence lengths $\xi_{\rm rms}$ of the neutron Cooper pairs as a function of the neutron Fermi momentum $k_{Fn}$ in both symmetric nuclear matter and pure neutron matter are drawn in the upper-right panel of Fig. 6. While $k_{Fn}$ decreases, the coherence lengths shrinks to $\sim 5$ fm at density of 0.4 fm$^{-1} < k_{Fn} < 0.8$ fm$^{-1}$ (0.4 fm$^{-1} < k_{Fn} < 0.9$ fm$^{-1}$) for symmetric nuclear (pure neutron) matter. Then it expands again at very low densities. These features can be understood as follows. In comparison with the virtual $S$-state in the vacuum, the neutron pairs feel an extra binding due to the pairing correlation as density increases; while at large $k_{Fn}$, the neutron pairs will strongly increase in size due to the Pauli principle. The difference of the coherence lengths between $\zeta = 0$ and $\zeta = 1$ at high densities is caused by the difference of the scalar mass $M^*$. When $k_{Fn} < 0.7$ fm$^{-1}$ ($k_{Fn} < 0.75$ fm$^{-1}$) for symmetric nuclear (pure neutron) matter, it is seen that the coherence length $\xi_{\rm rms}$ is smaller than the average inter-neutron distance $d_n$, which could be treated as the signature of the BCS–BEC crossover.

In order to characterize the spatial correlation of the neutron Cooper pairs, one can introduce the probability $P(r)$,

$$P(r) = \int_0^r \left|\Psi_{\rm pair}(r')\right|^2 r'^2\, dr', \tag{19}$$

which gives the probability for the pair partners within a relative distance $r$.

The probability $P(r)$ for the neutron pair partners correlated within $r = 3$ fm is shown in the upper-left panel of Fig. 6 as a function of $k_{Fn}$ in symmetric nuclear matter and pure neutron matter. It reaches the maximum value of about 0.75 around $k_{Fn} = 0.75$ fm$^{-1}$, and goes down at both lower or larger Fermi mo-

mentum. In the lower-left panel of Fig. 6, the probability $P(d_n)$, i.e., $P(r)$ for the pair partners within the average inter-neutron distance $r = d_n$, is plotted as well. The values of $P(d_n)$ increase monotonically with decreasing density, and approach to 1.0 at dilute area. From a regularized pairing model [45], it is suggested that the BCS–BEC crossover is determined by $P(d_n) > 0.807$ [29,30]. This limits the Fermi momentum $k_{Fn} < 0.7$ fm$^{-1}$ in symmetric nuclear matter and $k_{Fn} < 0.75$ fm$^{-1}$ in pure neutron matter for the realization of the BCS–BEC crossover.

The BCS–BEC crossover is also explored by the ratio $\Delta_{Fn}/e_{Fn}$ between the neutron pairing gap at the Fermi surface $\Delta_{Fn}$ and the neutron Fermi kinetic energy $e_{Fn} \equiv e(k_{Fn})$. If the ratio is large enough, the neutron pairing is expected to be in the strong coupling regime. From the regularized model, the BCS–BEC crossover region is estimated as $0.21 < \Delta_n/e_{Fn} < 1.33$ and the unitary limit is given at $\Delta_n/e_{Fn} = 0.69$ [29,30].

In the lower-right panel of Fig. 6, the ratios $\Delta_{Fn}/e_{Fn}$ plotted as a function of the neutron Fermi momentum are shown for both symmetric nuclear matter and pure neutron matter. As density decreases, the values grow up first and go into BCS–BEC crossover region at $k_{Fn} \sim 0.75$ fm$^{-1}$ for symmetric nuclear matter and $k_{Fn} \sim 0.8$ fm$^{-1}$ for pure neutron matter. It is found that the curves never intersect with the line of the unitary limit, namely, the neutron pairing does not go into the BEC regime. Then at very low densities with $k_{Fn} < 0.05$ fm$^{-1}$, the results decrease again and return back to the BCS region. Based upon the above analyses, the BCS–BEC crossover is marked in the density region with 0.05 fm$^{-1}$ $< k_{Fn} <$ 0.7 fm$^{-1}$ for the symmetric nuclear matter and 0.05 fm$^{-1}$ $< k_{Fn} <$ 0.75 fm$^{-1}$ for the pure neutron matter.

In conclusion, the di-neutron spatial correlations and the BCS–BEC crossover phenomenon for nuclear matter in the $^1S_0$ channel has been investigated based on the microscopic relativistic pairing theory with the effective RMF interaction PK1 in the *ph* channel and the realistic bare nucleon–nucleon interaction Bonn-B in the *pp* channel. It is found that the spatial structure of neutron Cooper pair wave function evolves continuously from BCS-type to BEC-type as density decreases, and a strong concentration of the probability density is revealed for the pair partners in the fairly small relative distance around 1.5 fm and the neutron Fermi momentum $k_{Fn} \in [0.6, 1.0]$ fm$^{-1}$, which is correlated with the di-neutron configuration in the surface of superfluid nuclei. In light of the evidence from the effective chemical potential, the quasiparticle excitation spectrum and the density correlation function, a true di-neutron BEC bound state does not occur at any density in nuclear matter. Neutron pairing is just in the transition region from BCS to BEC regime at low densities, and the most BEC-like state may appear at $k_{Fn} \sim 0.2$ fm$^{-1}$. From several characteristic quantities, such as the coherence length $\xi_{\rm rms}$, the probability $P(r)$ with $r = 3$ fm and $r = d_n$, and the ratio $\Delta_{Fn}/e_{Fn}$, the BCS–BEC crossover is found in the density region about 0.05 fm$^{-1}$ $< k_{Fn} <$ 0.7 fm$^{-1}$ for symmetric nuclear matter and 0.05 fm$^{-1}$ $< k_{Fn} <$ 0.75 fm$^{-1}$ for pure neutron matter. The results reveal a strong correlation of neutron pairs at such densities.

## Acknowledgements

B.S. acknowledges the support of FrontierLab@OsakaU Program for his three months stay in Osaka University, where part of this work has been performed. This work is partly supported by the Major State Basic Research Development Program (2007CB815000), and the National Natural Science Foundation of China (10975008 and 10775004).

## References

[1] J. Bardeen, L.N. Cooper, J.R. Schrieffer, Phys. Rev. 108 (1957) 1175.
[2] A.J. Leggett, J. Phys. (Paris) 41 (1980) C7.
[3] P. Nozières, S. Schmitt-Rink, J. Low Temp. Phys. 59 (1985) 195.
[4] Y. Ohashi, A. Griffin, Phys. Rev. Lett. 89 (2002) 130402.
[5] G.F.d. Téramond, B. Gabioud, Phys. Rev. C 36 (1987) 691.
[6] M. Baldo, J. Cugmon, A. Lejeune, U. Lombardo, Nucl. Phys. A 515 (1990) 409.
[7] T. Takatsuka, R. Tamagaki, Prog. Theor. Phys. Suppl. 112 (1993) 27.
[8] G.F. Bertsch, H. Esbensen, Ann. Phys. (N.Y.) 209 (1991) 327.
[9] J. Meng, P. Ring, Phys. Rev. Lett. 77 (1996) 3963.
[10] J. Meng, I. Tanihata, S. Yamaji, Phys. Lett. B 419 (1998) 1.
[11] J. Meng, P. Ring, Phys. Rev. Lett. 80 (1998) 460.
[12] T. Myo, S. Aoyama, K. Katō, K. Ikeda, Prog. Theor. Phys. 108 (2002) 133.
[13] A.B. Migdal, Yad. Fiz. 16 (1972) 427;
A.B. Migdal, Sov. J. Nucl. Phys. 16 (1973) 238.
[14] P.G. Hansen, B. Jonson, Europhys. Lett. 4 (1987) 409.
[15] M.V. Zhukov, B.V. Danilin, D.V. Fedorov, J.M. Bang, I.J. Thompson, J.S. Vaagen, Phys. Rep. 231 (1993) 151.
[16] Y.T. Oganessian, V.I. Zagrebaev, J.S. Vaagen, Phys. Rev. Lett. 82 (1999) 4996.
[17] F. Barranco, P. Bortignon, R.A. Broglia, G. Colò, E. Vigezzi, Eur. Phys. J. A 11 (2001) 385.
[18] K. Hagino, H. Sagawa, Phys. Rev. C 72 (2005) 044321.
[19] K. Hagino, N. Takahashi, H. Sagawa, Phys. Rev. C 77 (2008) 054317.
[20] F. Catara, A. Insolia, E. Maglione, A. Vitturi, Phys. Rev. C 29 (1984) 1091.
[21] M.A. Tischler, A. Tonina, G.G. Dussel, Phys. Rev. C 58 (1998) 2591.
[22] M. Matsuo, K. Mizuyama, Y. Serizawa, Phys. Rev. C 71 (2005) 064326.
[23] N. Pillet, N. Sandulescu, P. Schuck, Phys. Rev. C 76 (2007) 024310.
[24] F.V. De Blasio, M. Hjorth-Jensen, O. Elgarøy, L. Engvik, G. Lazzari, M. Baldo, H.-J. Schulze, Phys. Rev. C 56 (1997) 2332.
[25] M. Serra, A. Rummel, P. Ring, Phys. Rev. C 65 (2001) 014304.
[26] T. Nakamura, et al., Phys. Rev. Lett. 96 (2006) 252502.
[27] H. Esbensen, K. Hagino, P. Mueller, H. Sagawa, Phys. Rev. C 76 (2007) 024302.
[28] T. Myo, K. Katō, H. Toki, K. Ikeda, Phys. Rev. C 76 (2007) 024305.
[29] M. Matsuo, Phys. Rev. C 73 (2006) 044309.
[30] J. Margueron, H. Sagawa, K. Hagino, Phys. Rev. C 76 (2007) 064316.
[31] S.J. Mao, X.G. Huang, P.F. Zhuang, Phys. Rev. C 79 (2009) 034304.
[32] A.A. Isayev, Phys. Rev. C 78 (2008) 014306.
[33] K. Hagino, H. Sagawa, J. Carbonell, P. Schuck, Phys. Rev. Lett. 99 (2007) 022506.
[34] H. Kucharek, P. Ring, Z. Phys. A 339 (1991) 23.
[35] J. Li, B.Y. Sun, J. Meng, Int. J. Mod. Phys. E 17 (2008) 1441.
[36] R. Machleidt, Adv. Nucl. Phys. 19 (1989) 189.
[37] B. Serot, J.D. Walecka, Adv. Nucl. Phys. 16 (1986) 1.
[38] P. Ring, Prog. Part. Nucl. Phys. 37 (1996) 193.
[39] J. Meng, H. Toki, S.G. Zhou, S.Q. Zhang, W.H. Long, L.S. Geng, Prog. Part. Nucl. Phys. 57 (2006) 470.
[40] W. Long, J. Meng, N. VanGiai, S.-G. Zhou, Phys. Rev. C 69 (2004) 034319.
[41] Y. Sugahara, H. Toki, Nucl. Phys. A 579 (1994) 557.
[42] M. Baldo, U. Lombardo, P. Schuck, Phys. Rev. C 52 (1995) 975.
[43] M.M. Parish, B. Mihaila, E.M. Timmermans, K.B. Blagoev, P.B. Littlewood, Phys. Rev. B 71 (2005) 064513.
[44] B. Mihaila, S. Gaudio, K.B. Blagoev, A.V. Balatsky, P.B. Littlewood, D.L. Smith, Phys. Rev. Lett. 95 (2005) 090402.
[45] C.A.R. Sá de Melo, M. Randeria, J.R. Engelbrecht, Phys. Rev. Lett. 71 (1993) 3202.